

PAPER • OPEN ACCESS

Soil anisotropic stress-strain prediction using Normalised Rotational Multiple Yield Surface Framework (NRMYSF) for compacted tropical residual sandy soils

To cite this article: A Alias *et al* 2019 *IOP Conf. Ser.: Mater. Sci. Eng.* **527** 012018

View the [article online](#) for updates and enhancements.

Soil anisotropic stress-strain prediction using Normalised Rotational Multiple Yield Surface Framework (NRMYSF) for compacted tropical residual sandy soils

A Alias^{*1}, M J Md. Noor¹ and I B Mohamed Jais¹

¹ Faculty of Civil Engineering, Universiti Teknologi MARA, 40450 Shah Alam, Selangor, Malaysia

*Corresponding author email: asalasmidar@gmail.com

Abstract. Rotational Multiple Yield Surface Framework (RMYSF) is an anisotropic soil volume change model developed to integrate shear strength in characterising the soil volume change behaviour from the standpoint of the stress-strain response. The anisotropic soil volume change behaviour is described from the interaction between applied stress represented by the Mohr-Coulomb circle and shear strength in terms of curved-surface mobilized shear strength envelope. This research work is to enhance the current method of RMYSF using normalisation of axial strain to predict stress-strain behaviour. A series of triaxial tests has been conducted on Malaysian sedimentary sandy residual soil grade VI. The stress-strain curves and volume change behaviours were analysed using this enhanced method. Subsequently, the enhance method is apply to predict the soil stress strain respond and make comparison with the actual laboratory stress-strain curve. Essentially the normalised method of RMYSF has improved the accuracy of the prediction as presented in the paper.

1. Introduction

Residual soils are widely distributed in tropical region are formed from by the chemical and mechanical weathering of parent rocks at the location. Residual soil widespread more than 80% in Peninsular Malaysia [1] exhibit the characteristic of potential collapse upon wetting [2], [3], [4] and unsaturated behaviour [5].

[3] stated poor drainage conditions favour formation of montmorillonite-rich, expansive soils in semi-arid zones, while, good internal drainage favour the development of kaolinite dominant ferruginous soils in the sub-tropical zones. The ground water table found located at low level known as unsaturated or partially saturated zone, the boundary condition is a flux type hence issue concerning climatic changes (i.e. evaporation and infiltration), groundwater raise and reduction in negative pore pressure are inevitable [5]. As a result the soil shear strength and volume change along with hydraulic properties are responsive to climatic changes.

Unsaturated soil also exhibits volumetric instability to changes in water content. [1] explained moisture induced volumetric instability in residual soils manifest as swell (increase in void ratio upon water absorption), shrinkage (decrease in void ratio with reduction in water content) and collapse (reduction in void ratio upon saturation). This material also having collapse potential (massive sudden volume change), can undergo large settlements when wetted at overburden pressures bringing about damage to the overlying structures. Collapsible soil can bear a large applied vertical stress with small amount of compression, but then showed larger settlement when wet, with no rise in vertical stress [6].



Conversely, prediction of settlement is vital in foundation design and need to consider into account of unsaturated condition. Effective stress concept always been the norm framework in describing soil volume change behaviour [7] and those settlement models developed by this concept are empirical in nature. This model indicates at some point the settlement would stop because the soil becomes stiff enough due to being compressed to a closer particle arrangement, then compensate the loading. Furthermore, conventional models having the difficulties to explain the peculiar soil volume behaviour like inundation settlement.

[8] explained getting stiff is an indication of the increase in the strength, thus it is important to incorporate the role of shear strength in soil settlement behaviour. Rotational Multiple Yield Surface Framework (RMYSF) by [9] is a framework based on semi-empirical soil volume change model which applied the concept of effective stress and shear strength. The framework makes used the developed mobilised shear strength relation between the anisotropic compressions in the prediction of soil stress-strain behaviour. RMYSF established the relationship between the mobilised shear strength and the isotropic compression as the inherent property of the soil. This research used RMYSF to be attested against the volume change behavior of Semenyih sedimentary residual soil grade VI by conducting consolidated drained (CD) triaxial test.

2. Rotational Multiple Yield Surface Framework by the concept of effective stress and shear strength interaction

Shear strength according to total stress is referring to saturated state contrast to effective stress that relate to partially saturated. The two parameters defined the component in shear strength are frictional resistance of the soil particles (or angle of friction, ϕ) and cohesion of the soil, c . The variables describe the soil the soil maximum ability to resist shear stress under certain load.

According to [10] shear strength parameters affected by moisture content, pore pressure, structural influence, ground elevation, stress history, time, chemical reaction and environment. Well graded soils have high values of friction angle as reported by [11]. Researched by [12] showed the undrained shear strength is independent of change in total stress, except if the water content change thence concluded the water content is a function of the maximum principle stress. [13] explained the relationship between undrained shear strength and the quantity of water contained in soils could be expressed by nonlinear function. [14] described that the soil fabric plays an important role in the response of soil during shearing.

However, most of residual soil in Malaysia exhibit partially saturated condition therefore analysis using total stress become inadequate. The condition of effective stress can be achieved through saturation stage. During saturation, high cell pressures are applied which increases the moisture content and degree of saturation resulting in decreasing value of c' due to suction [15]. However [16] explained the saturation process does not change the value of angle of friction, ϕ' and the change in cohesion, c' is small. [17] explained total stress approach should be applied in the field only for the case where it can be assumed that the strength measured in the laboratory has relevance to the drainage conditions being simulated in the field. [17] further described in drained test, the pore pressure caused by the applied load are dissipated by allowing the pore fluids to flow in and out the soil specimen. The pore pressure at failure is known since it is controlled, and the stress state variables at failure can be used to analyse shear strength data [17].

Effective stress concept was introduced primarily by [7]. The concept characterize soil settlement base on the increase in the effective stress. However it was later realized that settlement do occur under effective stress decrease like the inundation settlement or wetting collapse [18]. Some of earlier works demonstrated the soil volume change models have been done by [7] and [19]. The models however consider the soil as elastic material which contradict the true nature of soil (i.e elasto-plastic material). Further researched by [20] and Modified Cam clay model [21] investigated critical state models for saturated soil which is not applicable to unsaturated soil, unable to explained inundation settlement. [22] utilized critical state models for unsaturated. The model was later refined twice by [23]. However, it was

found that the model unsuccessful to simulate volume change during alternate wetting and drying of unsaturated soils.

Alternatively, Rotational Multiple Yield Surface Framework (RMYSF) is a model to describe soil volume change that considering the true nature of soil. The framework satisfies these conditions;

- (1) developed from the standpoint of the soil stress-strain curves,
- (2) apply anisotropic stress condition,
- (3) incorporate effective stress as the driving variable,
- (4) incorporate the soil mobilized shear strength and,
- (5) apply the actual soil elastic-plastic response to stress.

The framework also explain inundation settlement or wetting collapse which occurs under effective stress decrease, massive settlement near saturation as reported and bigger inundation settlement under low net stress compared to higher net stress [8].

Conceptual model of RMYSF is the interaction of shear strength and effective stress. Shear strength defined by two parameters known as the angle of friction, ϕ and the cohesion of the soil, c . The mobilised shear strength envelope during compression acts as the resisting variable. [9] stated that the mobilised shear strength envelope taken as nonlinear envelope (i.e. curved surface envelope) is showing anticlockwise rotation about the origin towards the shear strength at failure. The increased value of mobilised angle of friction, ϕ_b indicates increase in shear strength shown in Figure 2. Shear plane is not developed during this stage as the compression is due to rearrangement of particle to a denser state.

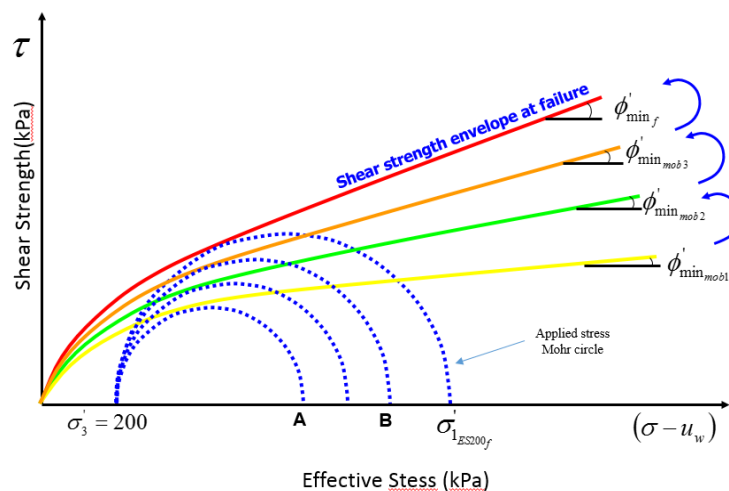


Figure 1. Rotational of the mobilised shear strength envelope due to enlargement of the effective stress Mohr-circle [8]

Effective stress is represented by Mohr circle which acts as the driving variable. The points of contact between driving (Mohr circle) and resisting variables (shear strength) established equilibrium condition, thus the settlement ceased. The effective stress (Mohr circle) is further observed to extend above current mobilised shear strength envelope as the strain increased. At this point, the driving variable exceeding resisting variable then the soil would experience further settlement. Further elaboration, the current mobilised envelope is acting as the yield surface. When the stress exceeds the current yield surface of the soil, the soil will undergo settlement. Mobilised shear strength, ϕ'_{min_mob} then change in position. The increase value of ϕ'_{min_mob} represents a specific degree of compression or axial strain, ϵ_a . The location of the mobilised shear strength envelope represents a specific degree of compression, irrespective of the effective stresses. [8] explained, there is a unique relationship between ϕ'_{min_mob} and ϵ_a irrespective of the effective stress applied. This behavior (i.e. mobilised shear strength and the corresponding axial strain) is consistent for the whole range of effective stress, thus indicates soil intrinsic property. The

inclination of the linear section for the shear strength envelope at failure represents the minimum friction angle at failure, ϕ'_{\min_f} . The yields surface rotates towards the failure envelope during compression as shown in Figure 2. The rotational movement is known as Rotational Multiple Yield Surface (RMYSF).

During compression, series of effective stress are applied to the soil. Mobilised shear strength enveloped then derived from stress-strain curves at different axial strain. This fulfilled the condition deriving soil behaviour from stress strain-curves. The stress-strain curves also show the soil plastic-elastic response to stress, when the soil reach maximum stress. The soil elastic-plastic characteristic is clearly shown rather than considering it fully elastic or plastic. The increase in rotational movement (i.e. $\phi'_{\min_{mob}}$ values) is due to increase in deviator stress. The $\phi'_{\min_{mob}}$ values are the shear strength parameter; indicates soil resisting variables in RMYSF's volume change behaviour model. Thence, the interaction of shear strength and effective stress is presented. The specimens tested in triaxial test subjected to anisotropic stress condition, where the vertical and horizontal stress are not equal. Condition is made to replicate the actual stress condition in the ground. As a result, RMYSF satisfied the five soil natural condition that has been discussed previously.

RMYSF uses actual stress-strain and effective values to define and predict volume change behaviour. However, the axial strains at failure are different depending on the effective stress of the specimens. Increase in effective stress result in increase in axial strain. Enhance analysis method of RMYSF by introducing normalised strain, where the stress-strain data are transform to maximum strain at failure by applying different factor. Normalisation is used to reach a linear, more robust relationship along with smoothing data, generalization of data and construct of new characteristic thus more accurate prediction data are offered. However, the reversion of data set is needed (using inverse factor) to compare the accuracy of prediction data with laboratory data. This method is known as Normalised Rotational Yield Surface Framework (NRMYSF).

Advancing the discussion of stress-strain relationship applying RMYSF, [24] stated a unique relationship is established between the minimum mobilized friction angle $\phi'_{\min_{mob}}$ and axial strain, ϵ_a . The relationship shows applying deviator stress rotates the mobilised shear strength into a new position regardless of the value of effective stress or net stress in accordance with axial strain either for saturation or unsaturation condition. [25] conducted consolidated drained triaxial compression tests for a given soil at various effective stress. From the results, they proposed an equation to determine the best fit curve for the minimum mobilised friction angle, $\phi'_{\min_{mob}}$, and axial strain ϵ_a which given in Equation 1. This relationship is able to predict the stress-strain response of a specific soil at every desired net stress or effective stress.

$$\phi'_{\min_{mob}} = \phi'_{\min_f} (1 - e^{-\Omega \epsilon_a}) \quad (\text{Eq. 1})$$

The Ω is the soil coefficient of anisotropic compression. Different soil has different graph of unique relationship. The coefficient Ω can be varied to determine the best representative curve for any soil types.

3. Test Soil and Experimental Procedures

Part of the land area of Malaysia comprises with residual sedimentary rock soil. The sedimentary soil was of sandstone origin of the Kenny Hill formation. The sedimentary rocks are inferred to be the Kenny Hill Formation comprising essentially sandstone, shale, phyllite and quartzite [26]. These soils are derived from sandstone, shale, schist formations and are generally more complex when compared to that of residual granitic soil. Overriding influence of parent material under alternate climate (hot and humid) is indicated by the high proportion of resistant minerals left in situ including ferric minerals [27]. [28] stated the products of chemical weathering are new, secondary minerals such as clay minerals and iron oxides / hydroxides (gibbsite, goethite, etc) which then remain as a part of the soil constituent.

The samples were taken at Semenyih, Hulu Langat district in Selangor with coordinates of 3°0'35.975"N; 101°51'51.145"E from a depth of 1.0m below the ground surface, to represent the original residual soil. Disturbed sample carefully placed in polyethylene bags to avoid moisture loss. The bags were tied properly and brought back to the soil laboratory on the same day. Original moisture values were recorded on site and then dry in the oven to determine the natural moisture content. All of the testings; physical and engineering properties and triaxial test following to [29].

The soil was reddish yellowish brown in colour and very friable. The soil was weathered sandstone of weathering VI and can be described as well-graded SAND according to the BSCS and SW according to USCS. The specific gravity of the soil was equal to 2.57. The initial moisture content was 22.3%, with values ranging from 20 % to 25 %. In the particle size distribution analyses, dry sieving were employed since there is less than 5% of fines exist within the residual soil. Based on the sieve analysis, the soil is well-graded SAND where sand particles are dominant at 72.4% summarised in Table 2. The physical properties of the soil are soil shown in Table 1.

Table 1. Soil Properties for Residual Soil from Semenyih

<i>Textural Composition</i>	<i>(%)</i>	<i>Soil Classification</i>	
Gravel	27.5	BSCS	Well-graded SAND
Sand	72.36	USCS	SW
Passing #200 (0.075)	5.0	Coefficient of uniformity, Cu	3.95
Passing #4 sieve and retained on #200	46	Coefficient of Curvature, Cg	0.59
<i>Physical Properties</i>		<i>Mechanical Properties</i>	
Natural Moisture Content (%)	22.3	Maximum Dry Density (Mg/m ³)	1.60
Specific Gravity	2.57	Optimum Moisture Content (%)	21.0
Liquid Limit (%)	48.0	Colour	Reddish yellowish brown
Plastic Limit (%)	28.2		
Plasticity Index (%)	19.8		

Experimental study was conducted using consolidated drained (CD) triaxial test in fully saturated condition on specimens with 50 mm diameter and 100 mm height. This gave the required height diameter ratio for the CD test of 2:1. Four (4) remoulded specimens were prepared at same moisture content and weight. Samples were first compacted at about 97% maximum dry density on the wet side of the Standard Proctor test at dry density of 1.56 Mg/m³. All samples were compacted in 1L compaction moulds following Standard Proctor test procedures. A 50 mm inside diameter steel tube with a bevelled sharp cutting edge were used to extrude columns of soil from the soil sample. The samples were then extruded and prepared for triaxial tests. All samples were carefully prepared to guarantee uniformity in term of moisture content and weight.

The samples were subjected to saturation stage, consolidation and compression at the rate of 0.01 mm/min. Effective stresses of 50 kPa, 100 kPa, 200 kPa and 300 kPa were applied to obtain Mohr circles which representing driving variables of the soil. Shear strength parameters of the tested soil were obtained following curved-surface envelope shear strength model (CSESSM) [9]. The analysis gave the values effective internal friction angle at failure, ϕ'_f , transition shear strength, τ_t and transition effective stress, $(\sigma-u_w)_t$. The transition net stress is the value of net or effective stress of which lesser than the envelope has non-linear form and beyond that it has its linear form. While the transition shear strength is the vertical height representing the strength that corresponds to transition net stress. The minimum friction angle is the inclination of the linear envelope from horizontal.

4. Stress-strain Response and Derivation of Mobilised Shear Strength Envelopes

The triaxial test has been conducted at different effective stresses of 50 kPa, 100 kPa, 200 kPa and 300 kPa. Stress-strain graphs were plotted to determine the effective internal friction angle at failure, ϕ'_f of specimens. Figure 2(a) shows the stress-strain relationship and the maximum value of deviator stress at failure. The maximum value recorded from the graph was 762 kPa. The values of effective stress and maximum deviator recorded at failure are used to draw Mohr circle envelope (Figure 2(b)). The curvilinear shear strength line is well fitted to Mohr circle as shown in Figure 2(b) using CSESSSM. The application of the curvilinear envelope manages to avoid any under-estimation or overestimation of the shear strength over the whole stress range [8]. The values of ϕ'_f , τ_t and $(\sigma-u_w)_t$ were determined and recorded in Table 2. Table 2 shows the effective internal friction angle at failure, ϕ'_f is 29.4° with transition shear strength, τ_t is 158 kPa and transition effective stress, $(\sigma-u_w)_t$ is 180 kPa.

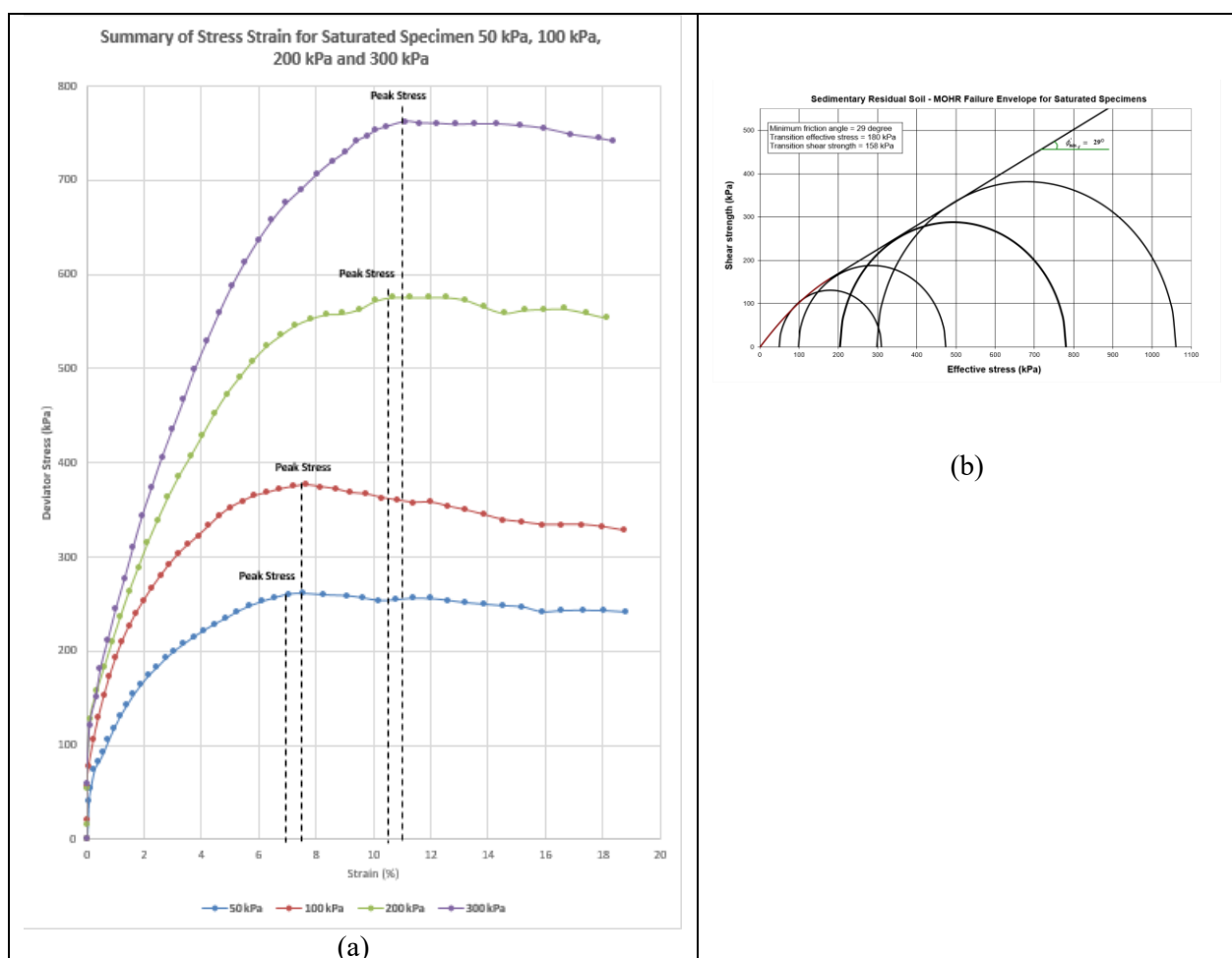


Figure 2. (a) Stress strain for saturated specimens at 50, 100, 200 and 300kPa effective stress while in (b) shows the non-linear shear strength envelope for saturated specimens.

Table 2. Effective shear stress parameters at failure for saturated specimens

Effective Stress, kPa	Condition of Failure			Shear Strength Parameters		
	DS (kPa)	PWP (kPa)	CP (kPa)	ϕ'_f	τ_t kPa	$(\sigma-U_w)_t$ kPa
50	262	351	400	29.4°	149	165
100	376	352	450			
200	576	346	550			
300	763	352	650			
DS – deviator stress	PWP – Pore Water Pressure			CP – Cell Pressure		

Obvious pattern during shearing stage, the maximum deviator stresses at failure respond at different value of axial strains, depend on the effective stress as shown in Figure 2(a). This research further examined to normalise data based on the maximum axial strain achieved at the final stage of shearing. The aim was to refine the unique relationship between the minimum mobilised friction angle and axial strain to be in unity, mean to converge each stage of effective stress will have the same axial strain at peak deviator stress. The value of strain at maximum deviator stress (i.e. 300 kPa) was selected. This value was used as numerator to normalise data for 50 kPa, 100 kPa and 200 kPa effective stress data. Figure 3 shows the stress-strain relationship with normalisation. Each set of data of effective stresses was multiply with certain factor in order to sort all peak deviator stresses become unity at the same axial stress. The maximum axial strain recorded was 11.126%.

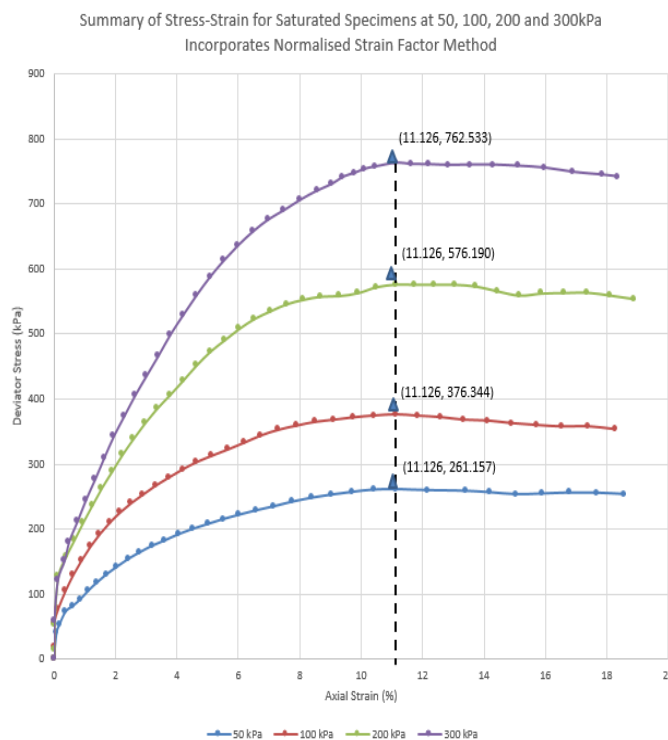


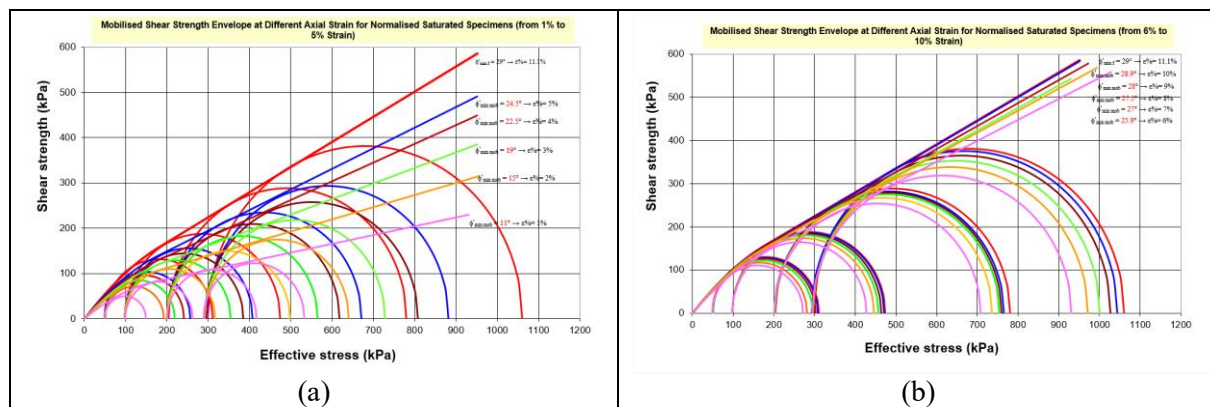
Figure 3. Peak deviator stress of each effective stress that have been normalised based on the highest peak deviator stress at 300kPa effective stress.

Table 3 presents normalised axial strain by multiplying using conversion factor 1.475, 1.45, 1.04 and 1 for 50, 100, 200 and 300kPa effective stress respectively. The deviator stress value corresponding to the normalised axial strain will remain from the experimental data (i.e. no conversion factor applied to deviator stress values).

Table 3. Normalised axial strain multiply by conversion factor for the deviator stress at effective stress of 50, 100, 200 and 300kPa

Normalised axial strain, %	Normalised conversion factor				Minimum mobilised friction angle $\phi'_{min_{mob}}$
	1.475 Dev. stress for 50kPa	1.45 Dev. stress for 100kPa	1.04 Dev. stress for 200kPa	1 Dev. stress for 300kPa	
1.00	110	163	163	212	11
2.00	150	221	221	289	15.5
3.00	175	258	258	360	19
4.00	195	286	286	418	22.5
5.00	215	320	320	460	24.5
6.00	225	340	340	495	25.9
7.00	235	361	361	524	27
8.00	245	365	365	534	27.5
9.00	250	374	374	555	28
10.00	260	383	383	565	29

The normalised minimum mobilised shear strength envelopes with the increase of deviator stress illustrated in Figure 4(a) and (b). The curvi-linear envelope were derived from deviator stresses from normalised stress-strain curves. The movement is showing anticlockwise rotation about the origin towards the shear strength at failure. Increase in $\phi'_{min_{mob}}$ indicates increase in shear strength. Each curvi-linear envelope depicts specific axial strain which correspond with specific minimum mobilised friction angle.

**Figure 4.** Mobilised shear strength envelope for saturated specimens at 50, 100, 200 and 300kPa effective stress (a) at 1%, 2%, 3%, 4% and 5% strain and (b) at 6%, 7%, 8%, 9%, 10% and 11% strain.

5. Prediction of stress-strain response using Normalised Multiple Yield Surface Framework (NMYSF)

Having this unique relationship (i.e. specific axial strain correspond to specific mobilised shear strength), the prediction of deviator stress can be done for any effective stress. Figure 5(a), (b), (c) and (d) show Mohr circles plotted for effective stress of 50kPa, 100kPa, 200kPa and 300 kPa in various axial strain. From the Mohr circles interacted with the curvi-linear envelopes, mobilised friction angles $\phi'_{min_{mob}}$ in various axial strains (i.e. 1% to 11%) were obtained. Apparently the graph nearly overlap each other's explaining mobilised shear strength envelopes rotate simultaneously during the application

of the deviator stress in the shearing stage irrespective of the magnitudes of the effective stress in the tests.

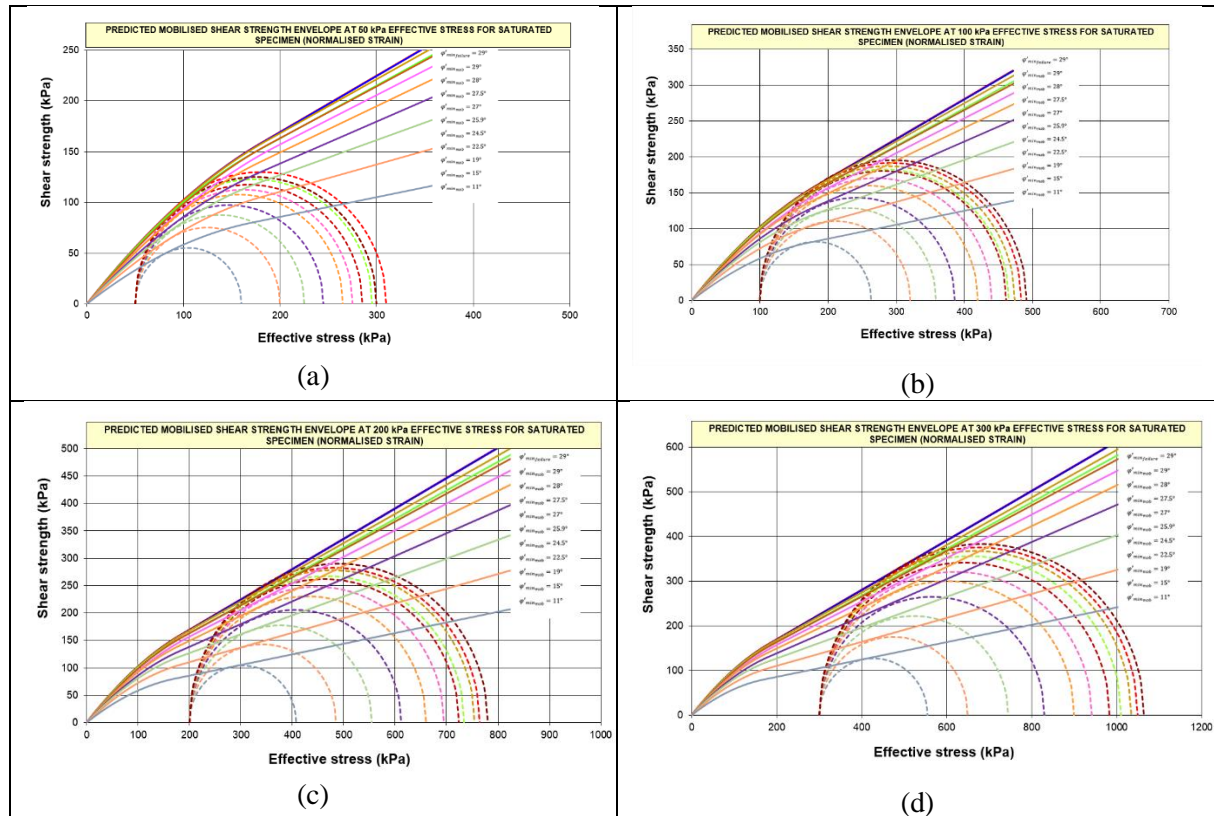


Figure 5. Predicted deviator stress of mobilised shear strength envelope (a) at 50kPa effective stress (b) at 100kPa effective stress (c) at 200kPa effective stress and (d) at 300kPa effective stress

The analyses gave the predicted deviator stress values for each effective stress that correspond to $\phi'_{min_{mob}}$ and axial strain. Table 4 is determined based on Figure 5 that presents the collected data with additional value of inverse normalised strain. The inversion is needed to compare the predicted data and laboratory data.

Table 4. Normalised axial strain with inverse factor and the predicted deviator stress at effective stress of 50, 100, 200 and 300kPa

Normalised axial strain, %	Actual axial strain for 50kPa	Predicted dev. stress for 50kPa	Actual axial strain for 100kPa	Predicted dev. stress for 100kPa	Actual axial strain for 200kPa	Predicted dev. stress for 200kPa	Actual axial strain for 300kPa	Predicted dev. stress for 300kPa
	Inverse factor							
	0.678		0.690		0.962		1.00	
1.00	0.678	110	0.690	160	0.962	207	1	212
2.00	1.356	150	1.380	217	1.923	285	2	289
3.00	2.034	175	2.070	258	2.885	355	3	360
4.00	2.712	195	2.760	286	3.846	417	4	418
5.00	3.390	215	3.450	320	4.808	460	5	460
6.00	4.068	225	4.140	340	5.769	495	6	495
7.00	4.745	235	4.830	361	6.731	524	7	524
8.00	5.423	245	5.519	365	7.692	534	8	534
9.00	6.101	250	6.209	374	8.654	555	9	555
10.00	6.779	260	6.899	383	9.615	565	10	565

Predicted stress-strain are plotted and compare with normalised axial strain-strain as shown in Figure 6(a). The comparison shows almost perfect fit. Predicted values are almost similar with laboratory value for all effective stress, the differences are very small. Figure 6(b) shows predicted inverse normalised strain with actual laboratory data. Predicted data fit almost perfectly within the line of the laboratory data. Table 7 shows the percentage accuracy for the predicted and experimental data.

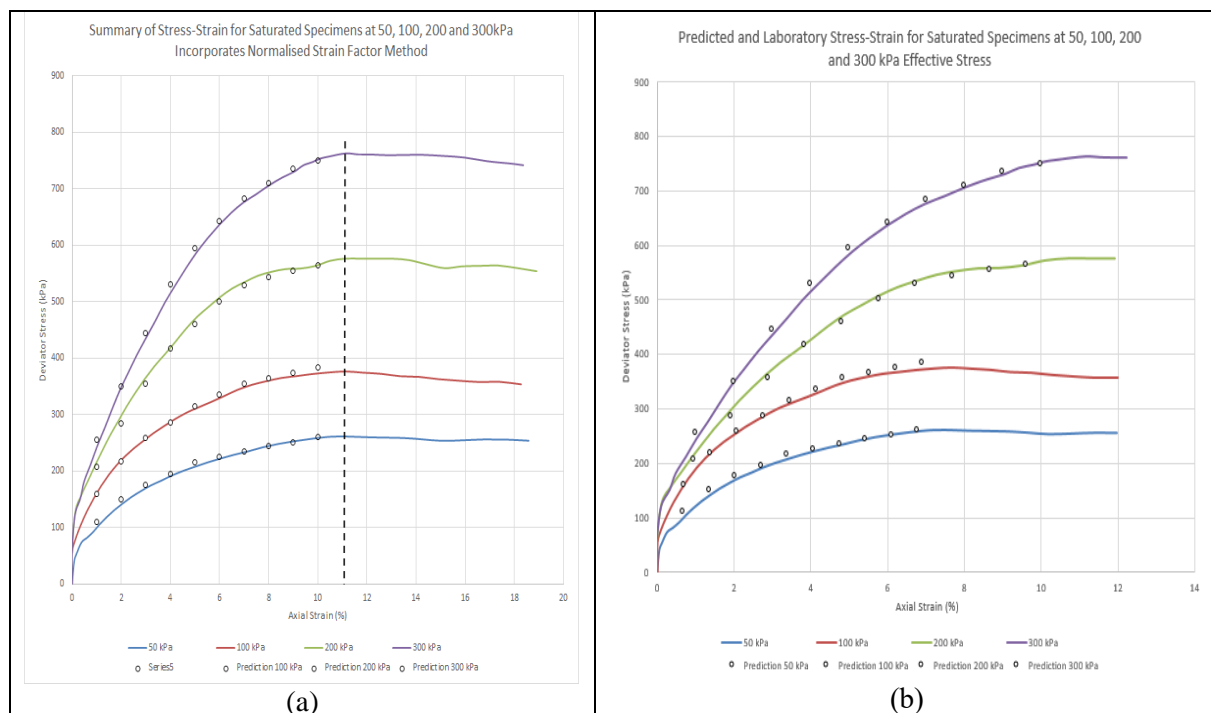
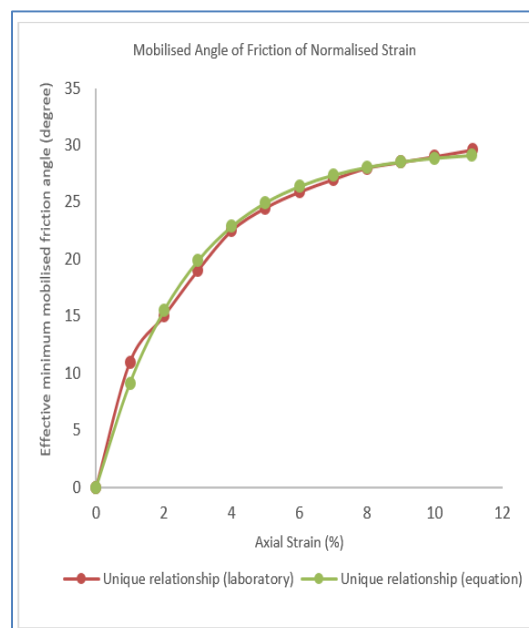
**Figure 6.** Prediction of stress-strain response at effective stress 50, 100, 200 and 300kPa (a) Normalised strain curve and (b) actual stress-strain curves

Table 5. Accuracy Analysis for Inverse Normalised Stress-Strain Plot and Laboratory Stress-Strain for 50kPa, 100kPa, 200kPa and 300kPa Effective Stress

Axial Strain (%)	Percentage Error (%) for 50kPa	Percentage Error (%) for 100kPa	Percentage Error (%) for 200kPa	Percentage Error (%) for 300kPa
1.00	9.88	0.69	4.14	5.59
2.00	6.65	0.92	4.11	0.47
3.00	3.36	0.72	2.80	2.17
4.00	2.18	0.42	0.92	2.87
5.00	3.54	3.16	1.55	2.39
6.00	1.54	3.06	2.44	0.86
7.00	0.80	3.68	1.95	0.95
8.00	0.05	1.41	3.18	0.54
9.00	1.01	1.79	0.46	0.66
10.00	0.60	2.78	0.03	0.30
Range of percentage error (%)	0.05 - 10	0.4 – 3.7	0.03 - 4	0.3 – 2.9
Mean absolute percentage error (%)	3.00	1.86	2.16	1.75

The range of percentage error is <1% to 10% as shown in Table 6. Lower percentage value indicates the prediction is practically similar to laboratory data. Data for 50kPa effective stress shows the highest range 0.5 – 10% but within accepted range. Good accuracy for normalised stress-strain were shown for 100kPa, 200kPa and 300kPa effective stress with percentage value less than 6% (Table 5). Table 5 shows the same pattern with lower percentage error at 4% for 100kPa, 200kPa and 300kPa effective stress, meaning the inverse normalised strain value give good match to actual laboratory data.

The data for each specific axial strain correspond to specific minimum mobilised friction angle, irrespective of effective stress is then plotted as illustrated in Figure 7. Fitting curve suggested by [25] is applied to obtain unique relationship for this Malaysian compacted tropical residual soil. The Ω value is 0.37 and it is the soil coefficient of anisotropic compression.

**Figure 7.** Mobilised Angle of Friction Normalised Strain and Unique Relationship

6. Conclusion

Rotational Multiple Yield Surface Framework (RMYSF) has the ability to make excellent prediction of the stress-strain response of Malaysian sedimentary sandy residual soil grade VI obtained from Semenyih Selangor Malaysia. The enhance method of RMYSF with the application of normalised axial strain technique has improved the prediction accuracy. Normalised axial strain is based on the maximum axial strain at the failure, where in this case is the test for 300kPa effective stress. The range of mean absolute percentage mean average less 4%, thus provide a good prediction accuracy compare with actually data recorded during experimental programme. The soil coefficient of anisotropy compression can be obtained using fitting curve that match the laboratory result.

7. References

- [1] Huat B B K, Aziz A A, Ali F, and Azmi N A 2008. Effect of Wetting on Collapsibility and Shear Strength of Tropical Residual Soil *Electrical Journal of Geotechnical Engineering (EJGE)*. Volume 13 2008 – Bundle G
- [2] Mansour Z, Chik Z, and Taha M R 2008 On Soil Collapse Potential Evaluation *International Conference on Construction and Building Technology*
- [3] Fookes P G 1990 *The quarterly journal of engineering geology report on tropical residual soils BGS 23: 103*
- [4] Barksdale R D and Blight G E 1997 Compressibility and settlements of residual soils *In Mechanics of Residual Soils, G.E. Blight (ed)*. Balkema. Rotterdam. 95-152
- [5] Ali F and Rahardjo H 2004 Unsaturated residual soil *In Huat, B.B.K et al., (eds) - Tropical Residual Soils Engineering Balkema Publisher*
- [6] Ahmed F A, Yahaya, A S and Farooq M A 2006 Characterization and geotechnical properties of Penang residual soils with emphasis on landslides *American Journal of Environmental Sciences, Vol. 2, No. 4, pp. 121-128*.
- [7] Terzaghi K 1943 *Theoretical soil mechanics* New York Wiley Publications
- [8] Md. Noor M J and Anderson W F 2015 Concept of Effective Stress and Shear Strength Interaction in Rotational Multiple Yield Surface Framework and Volume Change Behaviour of Banting Clay. Recent Advances in Applied and Theoretical Mechanics. *Proceeding of the 11th International Conference on Applied and Theoretical Mechanics (Mechanics' 15)*. Kuala Lumpur
- [9] Md Noor M J and Anderson W F 2006 A Comprehensive shear strength model for saturated and unsaturated Soils *Proc. 4th Int. Conf. on Unsaturated Soils, ASCE Geotechnical Special Publication, No. 147, Carefree, Arizona, Vol. 2. pp. 1992-2003*.
- [10] Cernica J N 1995 *Geotechnical engineering: soil mechanics* University of California, Wiley
- [11] Hawley P M 2001 Site Selection, Characterization, and Assessment. In: W.A. Hustrulid, M.K. McCarter and D.J.A. Van Zyl (Editors), *Slope Stability in Surface Mining. Society for Mining, Metallurgy*
- [12] Lambe T W and Whitman R V 1969 *Soil Mechanics* John Wiley & Sons, New York
- [13] Koumoto T and Houlsby G T 2001 Theory and practice of the fall cone test *Geotechnique, LI, No. 8, pp. 701-712*
- [14] Pineda J A and Colmenares J E 2006 Stress-strain suction behaviour of two clayey materials under unconfined conditions. *Proceeding of the 4th International Conference on Saturated Soils 2006 Vol. 1 1109-1120*
- [15] Fookes P G 1997 *Tropical residual soils* 1st ed London The Geological Society London.
- [16] Bressani L A and Vaughan P R 1989 Damage to soil structure during triaxial testing *Proceeding 12th Int. Conf. Soil Mech. and Found. Brookfield, Vt., pp. 17-20*.
- [17] Fredlund D G and Rahardjo H 1993 *Soil Mechanics for Unsaturated Soils* John Wiley and Sons, Inc, New York, 517

- [18] Blanchfield R and Anderson W F 2000 Wetting collapse in opencast coalmine backfill *Proceedings of the ICE Geotechnical Engineering*, London: 139-149.
- [19] Janbu N, Bjerrum L and Kjaernsli B 1956 Veiledring Ved Losning Av Fundermenteringsoppgaver *Norwegian Geotechnical Institute Publication No.16, Oslo*
- [20] Roscoe K H and Schofield A N 1963 Mechanical behavior of an idealized 'wet' clay *Proceeding European Conference on Soil Mechanics and Foundation Engineering, Wiesbaden (Essen: Deutsche Gessellschaft fur Erd-und Grundbau e.V.), vol. 1, pp. 47-54*
- [21] Roscoe K H and Burland J B 1968 On the Generalised Stress-Strain Behaviour of Wet Clay *In Heyman, J. and Leckie, F. A. (eds) Engineering Plasticity* Cambridge University Press. 535-609.
- [22] Alonso E E, Gens A, and Josa A 1990 A Constitutive Model for Partially Saturated Soil *Geotechnique* 40(3) 405-430
- [23] Wheeler S J and Sivakumar V 1995 An Elasto-plastic Critical State Framework for Unsaturated Soils. *Geotechnique* 53(1) 41-54
- [24] Saffari P, Md. Noor M J, Hadi B A, and Motamedi S 2014 *Laboratory Test Methods for Shear Strength Behavior of Unsaturated Soils Under Suction Control, Using Triaxial Apparatus* in InCIEC 2014, ed: Springer, 2015, pp. 567-576.
- [25] Mohamad Jais I B and Md. Noor M J 2010 Establishing unique relationship between minimum mobilised friction angle and axial strain for anisotropic soil settlement model. *In Unsaturated Soils: Theoretical and Numerical Advances in Unsaturated Soil Mechanics. Buzzzi, Fityus and Sheng (eds) Taylor & Francis Group, London, ISBN 978-0-415-80480-6.*
- [26] Omar R C, Jaafar R and Hassan H 1998 Engineering geology and earthwork problem associated with highway construction in soft soil at Sg. Rasau, Dengkil, Selangor. *Ninth Regional Congress on Geology, Mineral and Energy Resources of Southeast Asia - GEOSEA '98, pp. 175-186*
- [27] Juahir H H *Water quality data analysis and modeling of the Langat river basin, Thesis (PhD) Chapter 3. Faculty of Science, University of Malaya; 2009. Available: <http://dspace.fsktm.um.edu.my/handle/1812/507>.*
- [28] Tan B K 2004 Country case study: engineering geology of tropical residual soils in Malaysia *In Huat et.al (ed) Tropical Residual Soil Engineering* Balkema. Netherlands.
- [29] BS 1377 (1990) *Methods of Test for Soils for Civil Engineering Pusposes* British Standards Institution, London.

Acknowledgment

The authors would like to express their sincere gratitude to Ministry of Higher Education (MOHE) and Institute Research Management Institute (IRMI, UiTM) for providing financial support for this research. It was funded under Fundamental Research Grant Scheme (FRGS).